J. Biochem. 2012;151(4):391–401 doi:10.1093/jb/mvr146

JB THE JOURNAL OF BIOCHEMISTRY

Membrane-induced alteration of the secondary structure in the SWAP-70 pleckstrin homology domain

Received December 6, 2011; accepted December 15, 2011; published online January 13, 2012

Naomi Tokuda[1], Katsuhisa Kawai[1], Young-Ho Lee[2], Takahisa Ikegami[2], Satoru Yamaguchi[1], Hitoshi Yagisawa[1], Yasuhisa Fukui[3] and Satoru Tuzi[1,*]

[1]Graduate School of Life Science, University of Hyogo, Harima Science Garden City, Kouto 3-chome, Kamigori, Hyogo 678-1297, Japan, [2]Laboratory of Structural Proteomics, Institute for Protein Research, Osaka University, 3-2 Yamadaoka, Suita, Osaka 565-0871, Japan and [3]Institute of System and Cellular Medicine, National Health Research Institutes, 35 Keyan Road, Zhunan Town, Miaoli County 35053, Taiwan, Republic of China

*Satoru Tuzi, Graduate School of Life Science, University of Hyogo, Harima Science Garden City, Kouto 3-chome, Kamigori, Hyogo 678-1297, Japan. Tel: +81 791 58 0180, Fax: +81 791 58 0182, email: tuzi@sci.u-hyogo.ac.jp

Differences in the conformation of the pleckstrin homology (PH) domain of switch-associated protein-70 (SWAP-70) in solution and at the lipid bilayer membrane surface were examined using CD, fluorescence and NMR spectroscopy. Intracellular relocalization of SWAP-70 from the cytoplasm to the plasma membrane and then to the nucleus is associated with its cellular functions. The PH domain of SWAP-70 contains a phosphoinositide-binding site and a nuclear localization signal, which localize SWAP-70 to the plasma membrane and nucleus, respectively. CD and fluorescence spectra showed that a significant conformational alteration involving formation of disordered structure occurs when the PH domain binds to D-*myo*-phosphatidylinositol 3,4,5-trisphosphate or D-*myo*-phosphatidylinositol 4,5-bisphosphate embedded in lipid bilayer vesicles. NMR spectra indicate that Ala and Trp residues located in the C-terminal α-helix of the PH domain undergo conformational alterations to form a disordered structure at the vesicle surface. These conformational alterations were not induced by association with inositol 1,3,4,5-tetrakisphosphate in solution or coexistence of phosphatidylcholine vesicles. Interaction with the plane of the lipid bilayer via association with the phosphoinositides is required for the unfolding of the C-terminal α-helix of the PH domain. The unwinding of the C-terminal α-helix could regulate the functions of SWAP-70 at the plasma membrane surface.

Keywords: membrane surface/nuclear localization signal/PH domain/phosphatidylinositol 3,4,5-trisphosphate/switch-associated protein-70.

Abbreviations: NLS, nuclear localization signal; PH, pleckstrin homology; POPC, 2-oleoyl-1-palmitoyl-*sn*-glycero-3-phosphocholine; PtdIns(3,4,5)P_3, D-*myo*-phosphatidylinositol 3,4,5-trisphosphate; PtdIns(4,5)P_2, D-*myo*-phosphatidylinositol 4,5-bisphosphate; Ins(1,3,4,5)P_4, D-*myo*-inositol 1,3,4,5-tetrakisphosphate; SWAP-70, switch-associated protein-70; DTT, dithiothreitol; TMS, tetramethylsilane; BMRB, Biological Magnetic Resonance Data Bank; CP-MAS, cross polarization-magic angle spinning; DD-MAS, dipolar decoupled-magic angle spinning; Di-*O*-DMPC, 1,2-di-*O*-tetradecyl-*sn*-glycero-3-phosphocholine; DSS, 2,2-dimethyl-2-silapentane-5-sulphonate.

Switch-associated protein-70 (SWAP-70) is a 70 kDa protein originally identified as a part of the heavy-chain immunoglobulin class switching complex of B lymphocytes (*1*). SWAP-70 is also found in mast cells and in a variety of organs (*2*, *3*). It has been proposed that SWAP-70 contributes to cellular signal transduction pathways (in conjunction with a small G-protein known as Rac), and regulates cell motility through actin rearrangement (*3–5*). These molecular functions are thought to regulate cellular properties of B lymphocytes, mast cells, trophoblasts and malignant gliomas. Such properties include activation, migration, cell adhesion and invasion (*6–9*). Recent studies have reported a contribution of SWAP-70 to the transformation and invasion activity of mouse embryo fibroblasts (*10–12*). SWAP-70 is a multi-domain protein containing an EF-hand motif at the N-terminus, a pleckstrin homology (PH) domain in the central region and a coiled-coil domain at the C-terminus (*13*). SWAP-70 is recruited to the plasma membrane in response to cell stimulation and participates in cellular responses. In B lymphocytes, SWAP-70 is translocated into the nucleus after recruitment to the plasma membrane where it contributes to nuclear events (*13*). Both the phosphoinositide-binding site and the nuclear localization signal (NLS) have been reported to coexist in the PH domain (*13*). This suggests that the PH domain plays a pivotal role in functional relocalization of SWAP-70 in the cell.

The SWAP-70 PH domain has a typical PH domain tertiary structure consisting of a β-sandwich formed by seven anti-parallel β-strands and a C-terminal α-helix, which covers the open corner of the β-sandwich (Fig. 1) (*14–17*). Domains that share the PH domain structure are widely found in multi-domain proteins and participate in a variety of cellular functions such as signal transduction and cytoskeletal reorganization. The PH domain structure appears to provide a stable structural scaffold in a variety of proteins. The lipid-binding site for inositol polyphosphate-specific membrane binding (canonical lipid-binding site) is

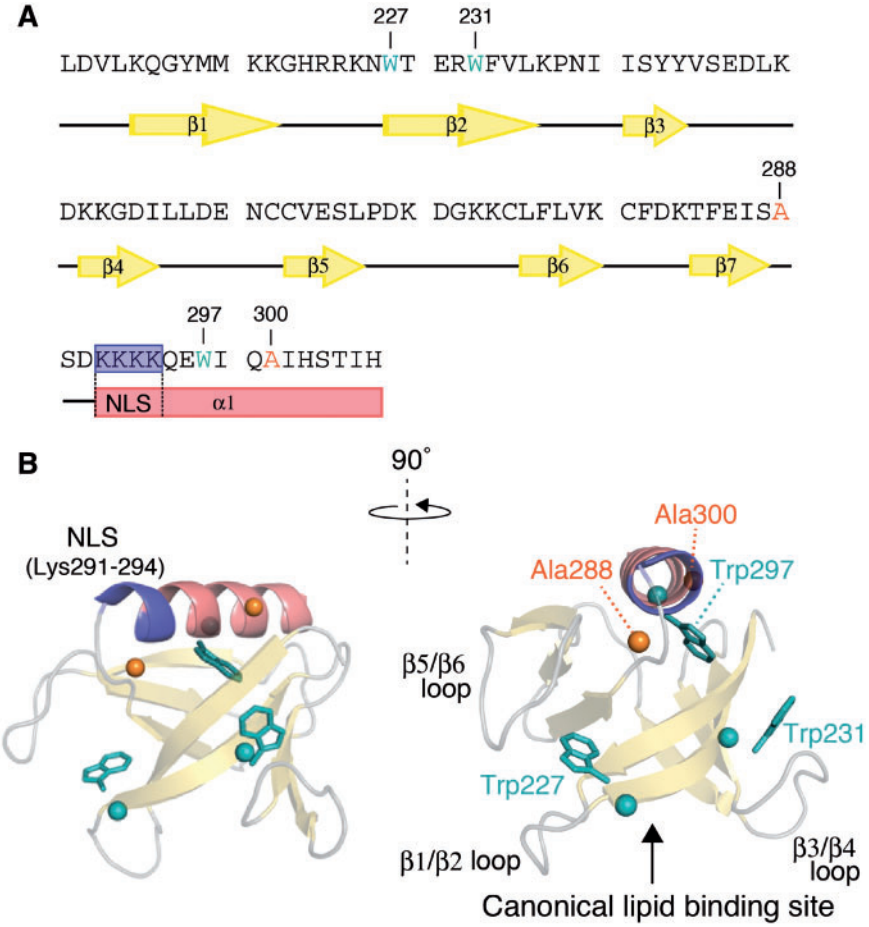

Fig. 1 Structure of the SWAP-70 PH domain. (A) The primary and secondary structures of the SWAP-70 PH domain (amino acids 209–306). The β-strands and the α-helix are indicated with yellow arrows and a red rectangle, respectively. NLS (Lys291–Lys294) is indicated by a blue rectangle. (B) Model structure of the SWAP-70 PH domain (PDB # 2DN6). The structure corresponding to amino acid residues 211–306 is indicated. The β-strands and the C-terminal α-helix are indicated with yellow arrows and a red helix. NLS in the α-helix is indicated in blue. ^{13}C labelled sites of Ala (orange), and Trp (cyan) residues are indicated with spheres, and the side chains of Trp residues are indicated by cyan sticks. Figures of the model structure were prepared using the PyMOL Molecular Graphics System, Version 1.3 (Schrödinger, LLC).

located between the loops connecting the β1- and β2-strands (β1/β2 loop) and the β3- and β4-strands (β3/β4 loop) at the unoccupied open corner of the β-sandwich (Fig. 1B) (*15*, *18*). SWAP-70 membrane localization is dominated by the affinity of the canonical lipid-binding site for the head group of D-*myo*-phosphatidylinositol 3,4,5-trisphosphate (PtdIns(3,4,5)P_3) (*19*). The monopartite NLS required for nuclear translocation of SWAP-70 has been identified as a sequence of four Lys residues located at the N-terminus of the C-terminal α-helix (Fig. 1). This cluster of Lys residues in the α-helix is a unique characteristic of the SWAP-70 PH domain (*13*).

To characterize the conformation of the PH domain at the lipid bilayer membrane surface, we investigated the conformational alteration of the PH domain at the vesicle surface by CD, fluorescence and NMR spectroscopy. CD and ^{13}C NMR spectra of the unliganded and vesicle-bound SWAP-70 PH domain revealed that remarkable conformational alterations occur at the C-terminal α-helix and that a disordered structure is formed at the vesicle surface. The secondary structural alterations of the PH domain induced at the lipid bilayer surface could contribute to the regulatory mechanism of the SWAP-70 functions at the plasma membrane surface such as the nuclear translocation of SWAP-70 initiated by exposure of the NLS sequence.

Materials and Methods

Materials

2-Oleoyl-1-palmitoyl-*sn*-glycero-3-phosphocholine (POPC) was purchased from Sigma (St Louis, MO, USA). D-*myo*-inositol 1,3,4,5-tetrakisphosphate (Ins(1,3,4,5)P_4), 1,2-dipalmitoyl-*sn*-glycero-3-phospho-(1-D-*myo*-inositol 3,4,5-trisphosphate) (PtdIns(3,4,5)P_3), 1,2-dipalmitoyl-*sn*-glycero-3-phospho-(1-D-*myo*-inositol 4,5-bisphosphate) (PtdIns(4,5)P_2) and DiC_6-PtdIns(3,4,5)P_3-agarose beads were purchased from Echelon Biosciences (Salt Lake City, UT, USA). 1,2-di-*O*-tetradecyl-*sn*-glycero-3-phosphocholine (Di-*O*-DMPC) was purchased from Avanti Polar Lipid (Birmingham, AL, USA). L-[3-^{13}C] alanine and L-[1-^{13}C] tryptophan were purchased from CIL (Andover, MA, USA). All reagents were used without further purification.

Protein expression and purification

The human SWAP-70 PH domain fragment (amino acids 209–306) was subcloned into a pGEX-2T-based bacterial expression vector (pGEX-2T from Amersham Bioscience, Piscataway, NJ, USA). The PH domain was expressed as a GST fusion protein in *Escherichia coli* (BL21). The bacteria were cultured in LB medium or M9 medium containing a mixture of 20 amino acids

(100 mg/l each). In this mixture, L-alanine or L-tryptophan was replaced by L-[3-^{13}C] alanine or L-[1-^{13}C] tryptophan, respectively. After induction for 5 h at 37°C with 0.1 mM isopropyl-1-thio-β-D-galacto-pyranoside, cells were harvested and sonicated in the presence of a mixture of proteinase inhibitors. The PH domain-GST fusion proteins were purified using glutathione-Sepharose 4B (GE Healthcare, Little Chalfont, UK). The PH domains were isolated by cleavage of the linker between the PH domain and GST by thrombin (Sigma) and purified by DEAE-Sepharose Fast Flow (GE Healthcare) chromatography. The final preparation of the SWAP-70 PH domain (molecular weight: 12,885) contains additional amino acid residues originating from a multi-cloning site of the expression vector, GSGGQG- and -GSPGIHRD, at the N- and C-termini of the natural amino acid sequence, respectively. The primary and secondary structures of the SWAP-70 PH domain are shown in Fig. 1A.

Estimation of binding affinity for phosphoinositides and Ins(1,3,4,5)P_4

The dissociation constants (K_d's) of the SWAP-70 PH domain for phosphoinositides (PtdIns(3,4,5)P_3 and PtdIns(4,5)P_2) embedded in POPC vesicles were evaluated using the PH domain-vesicle co-precipitation assay as reported previously (*20*). The affinity of the SWAP-70 PH domain for Ins(1,3,4,5)P_4 was estimated to determine the experimental conditions appropriate for spectroscopic measurements of the complex between the SWAP-70 PH domain and Ins(1,3,4,5)P_4. The interaction between the PH domain and Ins(1,3,4,5)P_4 was confirmed by measurement of competitive effect of Ins(1,3,4,5)P_4 on the PtdIns(3,4,5)P_3 binding of the PH domain. The PH domain-PtdIns(3,4,5)P_3-agarose beads co-precipitation assays were carried out in the presence of 0–100 μM of Ins(1,3,4,5)P_4 in solution. The PH domain was mixed with DiC_6-PtdIns(3,4,5)P_3-agarose beads or agarose beads in 20 mM potassium phosphate buffer (pH7.5) containing 0.025% NaN_3 and different concentrations of Ins(1,3,4,5)P_4 followed by incubation at room temperature for 15 min. The beads were washed and collected by centrifugation to be subjected to SDS–PAGE. The inhibitory effect of Ins(1,3,4,5)P_4 on the PH domain-PtdIns(3,4,5)P_3 binding was estimated from reduction in intensity of SDS–PAGE bands for the PH domain co-precipitated with PtdIns(3,4,5)P_3-agarose beads. In order to evaluate K_d for the PH domain-Ins(1,3,4,5)P_4 complex, the SWAP-70 PH domain and Ins(1,3,4,5)P_4 were mixed in 20 mM Tris buffer (pH 7.5). After incubation for 15 min at room temperature, <25% (volume) of the filtrate was separated from the solution by ultrafiltration using a Microcon YM-3 concentrator (molecular weight cut-off of 3,000) (Millipore, Billerica, MI, USA). The concentration of free Ins(1,3,4,5)P_4 in the filtrate containing Ins(1,3,4,5)P_4 and buffer was estimated by a quantitative phosphorus analysis (*21*). The K_d values for the phosphoinositides and Ins(1,3,4,5)P_4 were calculated from the following equation:

$$K_d = R\left\{[L]_0 - \frac{[PH]_0}{(R+1)}\right\} \quad (1)$$

where R = [PH]/[PH·L], [PH] is the concentration of the unliganded PH domain and [PH·L] is the concentration of the PH domain, which forms a complex with the ligand at equilibrium. $[PH]_0$ and $[L]_0$ are the total concentrations of the PH domain and the ligands accessible by the PH domain, respectively. We assumed that 70% of the phosphoinositides in the vesicles are exposed to the outer surface, based on the geometrical parameters of the vesicles as described in the previous work (*20*). The possible K_d range for Ins(1,3,4,5)P_4 is influenced by a shift in the binding equilibrium due to the removal of filtrate and was evaluated from the compositions of the PH domain-Ins(1,3,4,5)P_4 solution before and after of the ultrafiltration.

Preparation of PH domain samples

Unliganded SWAP-70 PH domains were dialysed with 20 mM potassium phosphate buffer (pH 7.5) containing 1 mM dithiothreitol (DTT) and 0.025% NaN_3. The SWAP-70 PH domains complexed with Ins(1,3,4,5)P_4 were prepared by mixing the PH domains in 20 mM potassium phosphate buffer (pH 7.5) containing 1 mM DTT and 0.025% NaN_3 with Ins(1,3,4,5)P_4. The SWAP-70 PH domains forming complexes with POPC/PtdIns(4,5)P_2, POPC/PtdIns(3,4,5)P_3 or Di-*O*-DMPC/PtdIns(3,4,5)P_3 vesicles were prepared by mixing the PH domains and vesicles in 20 mM potassium phosphate buffer (pH 7.5) containing 1 mM DTT and 0.025% NaN_3. POPC or Di-*O*-DMPC dissolved in chloroform was mixed with PtdIns(4,5)P_2 or PtdIns(3,4,5)P_3 in chloroform at a molar ratio of 95 : 5, and casted on glass to form a thin film. After evaporation of chloroform *in vacuo* for 1 day, the lipids were suspended in 20 mM potassium phosphate buffer (pH 7.5) containing 1 mM DTT and 0.025% NaN_3 to form vesicles, followed by three freeze-thaw cycles. For CD and fluorescence spectroscopy measurements, the vesicle suspensions were sonicated with a probe type sonicator for 15 min at 40°C before mixing with the PH domains to avoid scattering of light by large vesicles. The vesicle suspensions were incubated with PH domains for 15 min at room temperature to enable formation of the protein–vesicle complex.

Measurements of CD spectra

Far-UV CD spectra were recorded with a Jasco J-720WI spectropolarimeter in a 1-mm pathlength quartz cuvette at 25°C. Concentrations of the PH domains in the samples were adjusted to 0.2 mg/ml (15.5 μM).

Measurements of fluorescence spectra

Fluorescence spectra were recorded with a Horiba Jobin Yvon FluoroMax-4 spectrofluorometer at 25°C. Concentrations of the PH domains in the unliganded and POPC/PtdIns(3,4,5)P_3 vesicle-bound PH domain samples were adjusted to 5 μM. The emission spectra were recorded from 300 to 450 nm with excitation at 295 nm and slits of 2 and 2.5 nm for excitation and emission, respectively.

Measurements of ^{13}C NMR spectra

^{13}C NMR spectra were recorded on a Chemagnetics Infinity 400 spectrometer (^{13}C: 100.6 MHz). Single pulse excitation dipolar decoupled-magic angle spinning (DD-MAS) and cross polarization dipolar decoupled-magic angle spinning (CP-MAS) solid-state NMR were utilized to obtain high-resolution spectra for the PH domain–vesicle complexes with high apparent molecular weight. The spectral width was 40 kHz, the acquisition time was 51.2 ms and the repetition time was 4 s. Free induction decay profiles were acquired with 2,048 data points, and zero-filled to 32,768 data points prior to Fourier transformation. The π/2 pulse for carbon nuclei was 5 μs. The spinning rate for magic angle spinning was 2.6 or 4 kHz. A dipolar decoupling field strength of 55 kHz was applied to the vesicle-bound PH domain samples. A weaker ^{1}H irradiation field was applied to the unliganded PH domains and the PH domain/Ins(1,3,4,5)P_4 complexes in solution to decouple scalar couplings. The contact time for CP-MAS experiments was 1 ms. Transients were accumulated 40,000–60,000 times until a reasonable signal-to-noise ratio was achieved. ^{13}C chemical shifts were referenced to the carboxyl carbon signal of glycine micro-crystals grown from aqueous solution [176.03 ppm from tetramethylsilane (TMS)] and then expressed as relative shifts from TMS. The relative shift of the carbonyl carbon signal of glycine from the methyl carbon signal of 2,2-dimethyl-2-silapentane-5-sulphonate (DSS) was determined to be 178.33 ppm for microcrystalline glycine and aqueous solution of DSS (50 mM DSS in 20 mM potassium phosphate buffer (pH 7.5) containing 0.025% NaN_3) using the Chemagnetics Infinity 400 spectrometer at 25°C. The chemical shifts from TMS were converted to relative values from DSS by addition of 2.30 ppm when the chemical shifts obtained in this study were compared with the chemical shifts reported using solution NMR spectroscopy.

The unliganded ^{13}C-labelled PH domain was concentrated by ultrafiltration with Microcon YM-3 concentrators (Millipore) to achieve final concentrations of 2.33 mM. The Ins(1,3,4,5)P_4-bound ^{13}C-labelled PH domain was prepared by mixing Ins(1,3,4,5)P_4 with the PH domain to achieve the concentrations of the PH domain and Ins(1,3,4,5)P_4 of 2.33 and 2.66 mM, respectively. The vesicle-bound ^{13}C-labelled PH domains were prepared by mixing the PH domain with vesicles at the concentrations of the PH domain and PtdIns(3,4,5)P_3 at 0.233 and 0.582 mM, respectively, followed by concentration with ultracentrifugation at 541,000 *g* for 6 h at 4°C. The final concentration of the PH domains was ~4.3 mM. All preparations were packed into a 5-mm OD pencil-type zirconia rotor just prior to the NMR measurements. The rotors were sealed with epoxy resin to prevent dehydration.

Results

Kd's of the SWAP-70 PH domain–ligand complex

K_d's of the SWAP-70 PH domain for phosphoinositides embedded in POPC vesicles and Ins(1,3,4,5)P_4 in solution are summarized in Table I. The vesicle co-precipitation assay provides a K_d of $2.65 \pm 0.90\,\mu M$ for the complex of PH domain and PtdIns(3,4,5)P_3 in the vesicles. The PH domain also has affinity for PtdIns(4,5)P_2 in the vesicles with a K_d of $12.6 \pm 1.1\,\mu M$. This indicates that the SWAP-70 PH domain has the ability to bind either to PtdIns(3,4,5)P_3 or PtdIns(4,5)P_2 in the lipid bilayer, although the binding affinity for PtdIns(3,4,5)P_3 is higher than the affinity for PtdIns(4,5)P_2. The affinity of the PH domain for POPC vesicles containing no phosphoinositide is not detectable in the vesicle co-precipitation assay. Figure 2 shows SDS–PAGE bands for the PtdIns(3,4,5)P_3-agarose beads co-precipitation assay of the PH domain in the presence of 0, 5.0 and 100.0 μM of Ins(1,3,4,5)P_4 in solution. The PH domain co-precipitated with PtdIns(3,4,5)P_3-agarose beads was significantly decreased by the coexistence of 100.0 μM of Ins(1,3,4,5)P_4. This indicates that the Ins(1,3,4,5)P_4 interacts with the PH domain in a competitive manner with PtdIns(3,4,5)P_3 through the canonical lipid-binding sites, although the binding affinity for Ins(1,3,4,5)P_4 is significantly lower than that for PtdIns(3,4,5)P_3. The K_d for the PH domain–Ins(1,3,4,5)P_4 complex in Table I is determined from the free ligand concentration in the PH domain/Ins(1,3,4,5)P_4 solution as described in the experimental section. Since up to 25% (volume) of the solution was separated by ultrafiltration in order to determine the free ligand concentration, the binding equilibrium in the solution can be shifted due to the change in the PH domain and ligand composition during the experiment. The possible K_d range from 12.6 ± 3.3 to $30.3 \pm 9.5\,\mu M$ shown in Table I was estimated by taking into consideration this shift of equilibrium.

Table I. Binding affinity of SWAP-70 PH domain.

Ligand	Fraction of PH domain-ligand complex (%)[a]	K_d (μM)[a]
Ins(1,3,4,5)P_4[b]	61.2 ± 3.6	12.6 ± 3.3
	-47.4 ± 5.4[c]	-30.3 ± 9.5[c] (5)[d]
POPC/PtdIns(3,4,5)P_3[e]	74.4 ± 4.9	2.65 ± 0.90 (10)[d]
POPC/PtdIns(4,5)P_2[e]	46.2 ± 1.7	12.6 ± 1.1 (6)[d]
POPC[f]	ND[g]	–

[a]Values are mean ± SD ($P < 0.05$). [b]Total concentrations of both PH domain and Ins(1,3,4,5)P_4 are 50.0 μM. [c]Possible ranges of fraction and K_d originate from removal of filtrate are shown. [d]Number of experiments. [e]Total concentrations of PH domain, lipids and accessible phosphoinositide are 11.5, 460 and 16.1 μM, respectively. [f]Total concentrations of PH domain and POPC are 11.5 and 460 μM, respectively. [g]Not detectable.

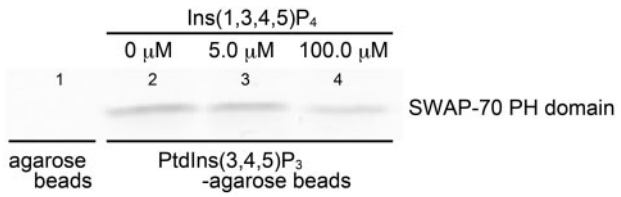

Fig. 2 Binding of the SWAP-70 PH domain to PtdIns(3,4,5)P_3-agarose beads in the presence of Ins(1,3,4,5)P_4. SDS–PAGE bands of the SWAP-70 PH domain bound to agarose beads in the absence of Ins(1,3,4,5)P_4 (lane 1), PtdIns(3,4,5)P_3-agarose beads in the presence of 0 (lane 2), 5.0 (lane 3) and 100.0 μM (lane 4) of Ins(1,3,4,5)P_4. Concentrations of the PH domain and PtdIns(3,4,5)P_3 are 3.88 and 5.0 μM, respectively.

CD spectra of the SWAP-70 PH domain

Far-UV CD spectroscopy was employed to investigate differences in the secondary structure of the PH domain in the presence and absence of vesicles. The spectral range <205 nm is not shown because the signal-to-noise ratio is low in this area. The black lines in the upper panels of Fig. 3A–C are CD spectra of the unliganded SWAP-70 PH domain. Each spectrum is characterized by a negative value in the region between 205 and 235 nm with negative peaks at ~210 and 220 nm. These characteristics are consistent with the model structure of the unliganded PH domain determined in solution (Fig. 1B) with a well-defined tertiary structure consisting of the seven-stranded β-sandwich and C-terminal α-helix. The red dotted line in the upper panel of Fig. 3A is a spectrum of the PH domain in the presence of Ins(1,3,4,5)P_4. The ratio of the PH domain that forms a complex with Ins(1,3,4,5)P_4 was estimated from Eq. 1 using the K_d of the PH domain–Ins(1,3,4,5)P_4 complex (Table I), the total concentration of the PH domain (15.5 μM) and the total concentration of Ins(1,3,4,5)P_4 (155 μM). It was estimated that 82.4% of the PH domains form complexes when the K_d value of 30.3 μM (Table I) was used. A difference spectrum generated from spectra of the Ins(1,3,4,5)P_4-bound and unliganded PH domains is shown in the lower panel of Fig. 3A. The absence of significant differences in the spectra indicates that there are no conformational alterations of the PH domain induced by binding to Ins(1,3,4,5)P_4. Blue and green lines in the upper panel of Fig. 3B are the spectra of the SWAP-70 PH domain bound to POPC/PtdIns(3,4,5)P_3 and POPC/PtdIns(4,5)P_2 vesicles, respectively. Ratios of the PH domains bound to phosphoinositides were estimated from Eq. 1 using K_ds for PtdIns(3,4,5)P_3 and PtdIns(4,5)P_2 in the vesicles shown in Table I and total concentrations of the PH domain (15.5 μM) and the surface exposed phosphoinositides (66.1 μM). About 95.1 and 80.9% of the PH domains were estimated to form complexes with PtdIns(3,4,5)P_3 and PtdIns(4,5)P_2 in the vesicles, respectively. The blue line in the lower panel of Fig. 3B is a difference spectrum between the POPC/PtdIns(3,4,5)P_3 vesicle-bound and unliganded PH domains. There is an increase in the negative value at shorter wavelengths <220 nm and a negative peak centred at 232 nm. These features are induced by binding to the POPC/PtdIns(3,4,5)P_3 vesicles. The increase in the negative value in the region between 205 and 210 nm indicates the formation of a disordered structure. Similar changes in the

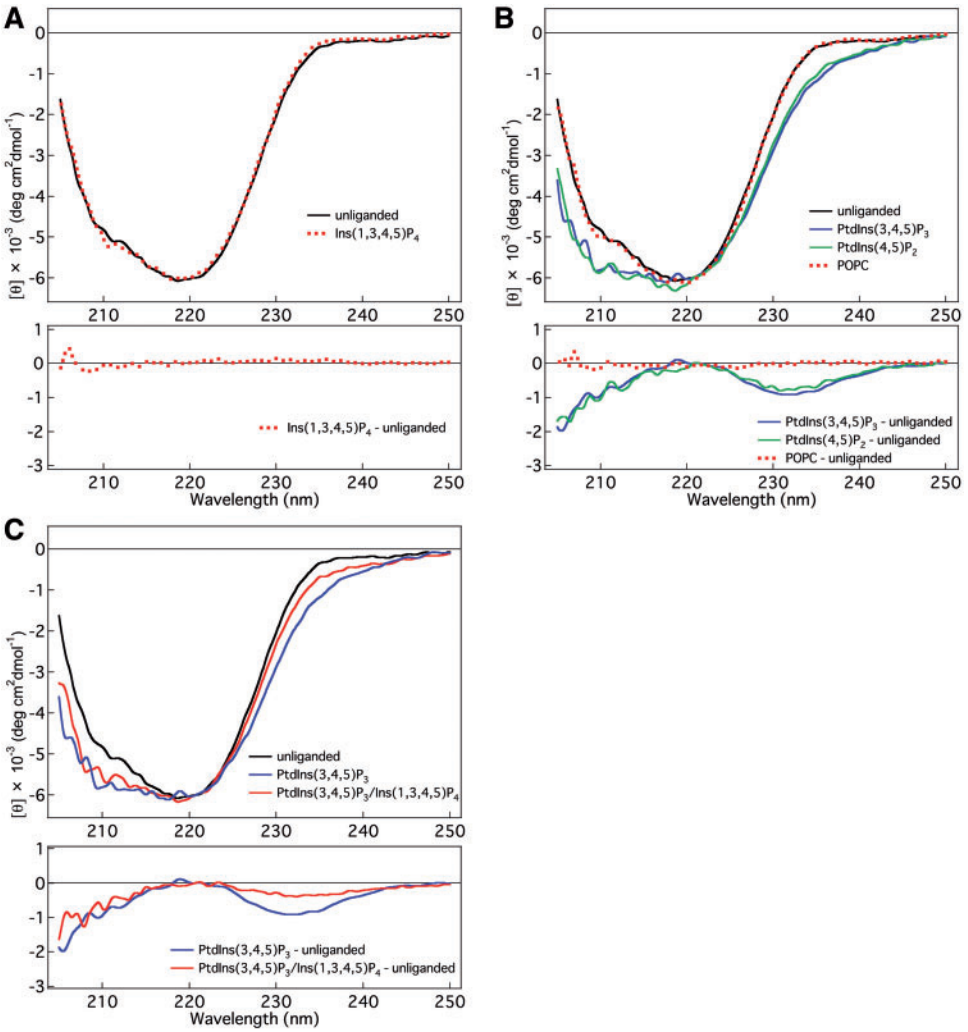

Fig. 3 CD spectra of the SWAP-70 PH domain. (A) Upper panel: spectra of unliganded (black line: unliganded) and Ins(1,3,4,5)P_4-bound [red-dotted line: Ins(1,3,4,5)P_4] PH domains. Concentrations of PH domain and Ins(1,3,4,5)P_4 are 15.5 and 155 μM, respectively. Lower panel: difference spectrum between Ins(1,3,4,5)P_4-bound and unliganded PH domains [red-dotted line: Ins(1,3,4,5)P_4-unliganded]. (B) Upper panel: spectra of unliganded (black line: unliganded), POPC/PtdIns(3,4,5)P_3 vesicle-bound [blue line: PtdIns(3,4,5)P_3], POPC/PtdIns(4,5)P_2 vesicle-bound [green line: PtdIns(4,5)P_2] PH domains and PH domain in the presence of POPC vesicles (red-dotted line: POPC). Concentrations of PH domain and accessible phosphoinositides are 15.5 and 66.1 μM, respectively. The total concentration of lipid in the vesicles is 1.89 mM. Lower panel: difference spectra between POPC/PtdIns(3,4,5)P_3 vesicle-bound and unliganded PH domains [blue line: PtdIns(3,4,5)P_3-unliganded], POPC/PtdIns(4,5)P_2 vesicle-bound and unliganded PH domains [green line: PtdIns(4,5)P_2-unliganded] and PH domains in the presence and absence of POPC vesicles (red-dotted line: POPC-unliganded). (C) Upper panel: spectra of unliganded PH domain (black line: unliganded) and POPC/PtdIns(3,4,5)P_3 vesicle-bound PH domains in the absence [blue line: PtdIns(3,4,5)P_3] and presence [red line: PtdIns(3,4,5)P_3/Ins(1,3,4,5)P_4] of Ins(1,3,4,5)P_4. Concentrations of PH domain and accessible PtdIns(3,4,5)P_3 are 15.5 and 66.1 μM, respectively. The concentration of Ins(1,3,4,5)P_4 is 1.32 mM. Lower panel: difference spectra between POPC/PtdIns(3,4,5)P_3 vesicle-bound and unliganded PH domains in the absence [blue line: PtdIns(3,4,5)P_3-unliganded] and presence [red line: PtdIns(3,4,5)P_3/Ins(1,3,4,5)P_4-unliganded] of Ins(1,3,4,5)P_4.

CD spectrum are shown in the difference spectrum between the POPC/PtdIns(4,5)P_2 vesicle-bound and unliganded PH domains in the lower panel of Fig. 3B (green line). The red-dotted line in the upper panel of Fig. 3B is a spectrum of the PH domain in the presence of the POPC vesicles at the same lipid concentration used in the samples containing POPC/PtdIns(3,4,5)P_3 or POPC/PtdIns(4,5)P_2 vesicles. A difference spectrum between the PH domains in the presence and absence of the POPC vesicles (red-dotted line in the lower panel of Fig. 3B) shows that the conformation of the PH domain is unaffected by the coexistence of the POPC vesicles. The red and blue lines in the upper panel of Fig. 3C are spectra of the PH domains bound to the POPC/PtdIns(3,4,5)P_3 vesicles in the presence and absence of 1.32 mM of Ins(1,3,4,5)P_4, respectively. Difference spectra between the vesicle-bound and unliganded PH domains in the presence and absence of Ins(1,3,4,5)P_4 are shown as red and blue lines, respectively, in the lower panel of Fig. 3C. The decreases in the intensity of the negative values in the red line compared with the blue line reveal that the coexistence of Ins(1,3,4,5)P_4 suppresses the conformational alterations in the PH domain, which are induced by the POPC/PtdIns(3,4,5)P_3 vesicles.

Fluorescence spectra of the Trp residues in the SWAP-70 PH domain

The black lines in Fig. 4A and C are fluorescence spectra of Trp residues in the unliganded SWAP-70 PH domain. Three Trp residues in the SWAP-70 PH domain (Trp227, Trp231 and Trp297) give rise to a fluorescence emission maximum at 332 nm. The green-dotted and red-dashed lines in Fig. 4A are spectra of the PH domain in the presence of Ins(1,3,4,5)P_4 and POPC vesicles, respectively. The ratio of the PH domain that forms a complex with Ins(1,3,4,5)P_4 was estimated from Eq. 1 using the K_d of the PH domain-Ins(1,3,4,5)P_4 complex (Table I) and the total concentrations of the PH domain (5.0 μM) and Ins(1,3,4,5)P_4 (50 μM). In total of 60.8% of the PH domains were estimated to form the complexes when a K_d value of 30.3 μM (Table I) was used. The lipid concentration of the POPC vesicles was adjusted to the total concentration of lipids in the samples containing POPC/PtdIns(3,4,5)P_3 or POPC/PtdIns(4,5)P_2 vesicles. The intensities of the spectra in Fig. 4A were normalized at 332 nm to facilitate the comparison. Differences in intensity among the original spectra are likely due to fading of the chromophore. These differences approached 11% of the intensity of the black line at 332 nm. As shown in Fig. 4A, the presence of Ins(1,3,4,5)P_4 and the POPC vesicles does not induce any differences in the emission maxima and the shape of the fluorescence spectra. This indicates that the environments around the Trp side chains in the PH domain are unaffected by binding of Ins(1,3,4,5)P_4 and the non-specific interaction with POPC vesicles. The red line and the blue-dotted line in Fig. 4B are spectra of the PH domains bound to the POPC/PtdIns(3,4,5)P_3 and POPC/PtdIns(4,5)P_2 vesicles, respectively. The ratios of the PH domains bound to phosphoinositides were estimated from Eq. 1 using K_ds for PtdIns(3,4,5)P_3 and PtdIns(4,5)P_2 in the vesicles shown in Table I and the total concentrations of the PH domain (5.0 μM) and the surface exposed phosphoinositides (56.0 μM). About 95.1 and 80.5% of the PH domains were estimated to form complexes with PtdIns(3,4,5)P_3 and PtdIns(4,5)P_2 in the vesicles, respectively. The intensities of the spectra in Fig. 4B were normalized at 334 nm. The difference in the intensity between the unnormalized spectra was 4% of the intensity of the red line at 334 nm. The spectra of the PH domain bound to POPC/PtdIns(3,4,5)P_3 and POPC/PtdIns(4,5)P_2 vesicles give rise to identical fluorescence spectra with emission maxima at 334 nm. Unnormalized spectra of the POPC/PtdIns(3,4,5)P_3 vesicle-bound PH domain (red line), the unliganded PH domain (black line) and a difference spectrum between these spectra (red-dotted line) are shown in Fig. 4C. The binding to PtdIns(3,4,5)P_3 induces a red shift of the fluorescence maximum from 332 to 334 nm. This is accompanied by a reproducible significant increase in fluorescence intensity. A positive peak in the difference spectrum with a maximum at 339 nm shows an increase in fluorescence emission centred at 339 nm. The red shift of the fluorescence maximum of the PH domain due to vesicle binding suggests that there is an increase in molecular reorganization in the vicinity of

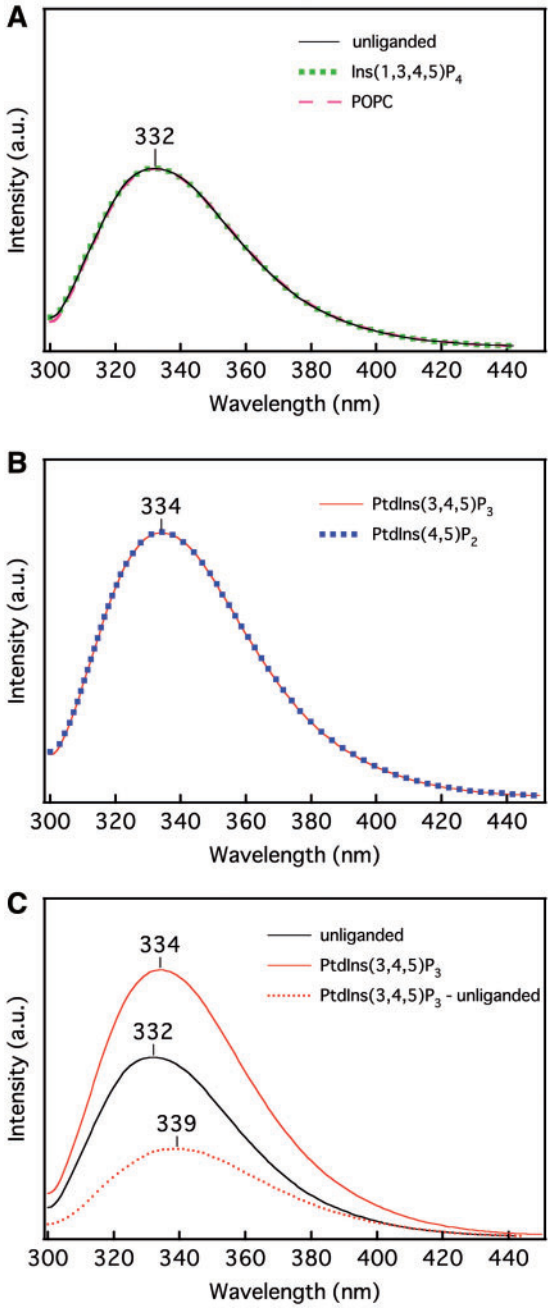

Fig. 4 Fluorescence spectra of the SWAP-70 PH domain. (A) Fluorescence spectra of unliganded PH domain (black line: unliganded), Ins(1,3,4,5)P_4-bound PH domain [green dotted line: Ins(1,3,4,5)P_4] and PH domain in the presence of POPC vesicles (red-dashed line: POPC).The intensities of the spectra were normalized at 332 nm. Concentrations of PH domain, Ins(1,3,4,5)P_4 and POPC are 5.0 μM, 50 μM and 1.6 mM, respectively. (B) Spectra of POPC/PtdIns(3,4,5)P_3 vesicle-bound [red line: PtdIns(3,4,5)P_3] and POPC/PtdIns(4,5)P_2 vesicle-bound [blue-dotted line: PtdIns(4,5)P_2] PH domains. The intensities of the spectra were normalized at 334 nm. Concentrations of PH domain and accessible phosphoinositides are 5.0 μM and 56.0 μM, respectively. (C) Unnormalized spectra of unliganded (black line: unliganded) and POPC/PtdIns(3,4,5)P_3 vesicle-bound [red line: PtdIns(3,4,5)P_3] PH domains, and a difference spectrum between POPC/PtdIns(3,4,5)P_3 vesicle-bound and unliganded PH domains [red-dotted line: PtdIns(3,4,5)P_3-unliganded]. The concentrations of PH domain and PtdIns(3,4,5)P_3 are 5.0 μM and 56.0 μM, respectively.

the Trp side chains in the vesicle-bound state. The increase in fluorescence emission at the vesicle-bound state could be a result of separation of the Trp side chains from quenchers via conformational alterations and/or interactions with the hydrophobic layer of the lipid bilayer.

^{13}C NMR spectra of the [3-^{13}C]Ala-labelled SWAP-70 PH domain

Figure 5A shows a ^{13}C NMR spectrum of the unliganded [3-^{13}C]Ala-labelled SWAP-70 PH domain in solution. The ^{13}C-labelled side chain methyl groups of two alanine residues, Ala288 and Ala300, give rise to peaks at 18.6 and 15.9 ppm, respectively. Ala300 is located in the C-terminal α-helix and Ala288 is located at the C-terminus of the β7-strand adjacent to the C-terminal α-helix in the model structure of the unliganded SWAP-70 PH domain in solution (Fig. 1). Peak assignments are based on the reported assignment of the solution ^{13}C NMR spectrum utilized for constructing the 3D model structure [Biological Magnetic Resonance Data Bank (BMRB) # 10319]. Figure 5B shows a ^{13}C NMR spectrum of the [3-^{13}C]Ala-labelled SWAP-70 PH domain in the presence of Ins(1,3,4,5)P_4. According to the K_d of the PH domain-Ins(1,3,4,5)P_4 complex (Table I) and total concentrations of the PH domain (2.33 mM) and Ins(1,3,4,5)P_4 (2.66 mM) in solution, it is estimated from Eq. 1 that 94.0% of the PH domains form complexes when a K_d of 30.3 μM was used. The spectrum is virtually identical to that of the unliganded PH domain except for a slight upfield shift of the Ala288 signal to 18.5 ppm. Figure 5C and D shows the DD-MAS and CP-MAS ^{13}C NMR spectra of the [3-^{13}C]Ala-labelled SWAP-70 PH domain bound to PtdIns(3,4,5)P_3 embedded in the POPC/PtdIns(3,4,5)P_3 vesicles. The ratio of the PH domain bound to PtdIns(3,4,5)P_3 was estimated from Eq. 1 using the K_d for PtdIns(3,4,5)P_3 in the vesicles (Table I) and total concentrations of the PH domain (0.233 mM) and PtdIns(3,4,5)P_3 (0.582 mM) in the mixture. In total of 96.2% of the PH domains in the sample were estimated to form complexes with vesicles when 50% of PtdIns(3,4,5)P_3 is exposed to the outer surface of the vesicles. The PH domain–vesicle complex was collected by ultracentrifugation to achieve a final concentration of the PH domain of ~4.3 mM. In Fig. 5C and D, the asterisks indicate signals from lipid molecules. A chemical shift of the peak at 15.9 ppm in the DD-MAS spectrum (Fig. 5C) coincides with that of Ala300 (15.9 ppm) in solution (Fig. 5A). Peaks at 21.2 and 16.7 ppm in Fig. 5C have no equivalent in the spectra in solution (Fig. 5A and B). These peaks indicate the emergence of novel conformations of Ala residues at the vesicle surface. Solid state ^{13}C NMR studies of conformation-dependent chemical shifts of Ala residues in synthetic polypeptides and proteins have shown that the chemical shift displacement of the side chain methyl carbon is sensitive to the secondary structure (*22*). Quantum mechanical calculations also support the existence of a relationship between the secondary structure and the chemical shift of the Ala residues (*23*). The methyl carbon signal of the Ala

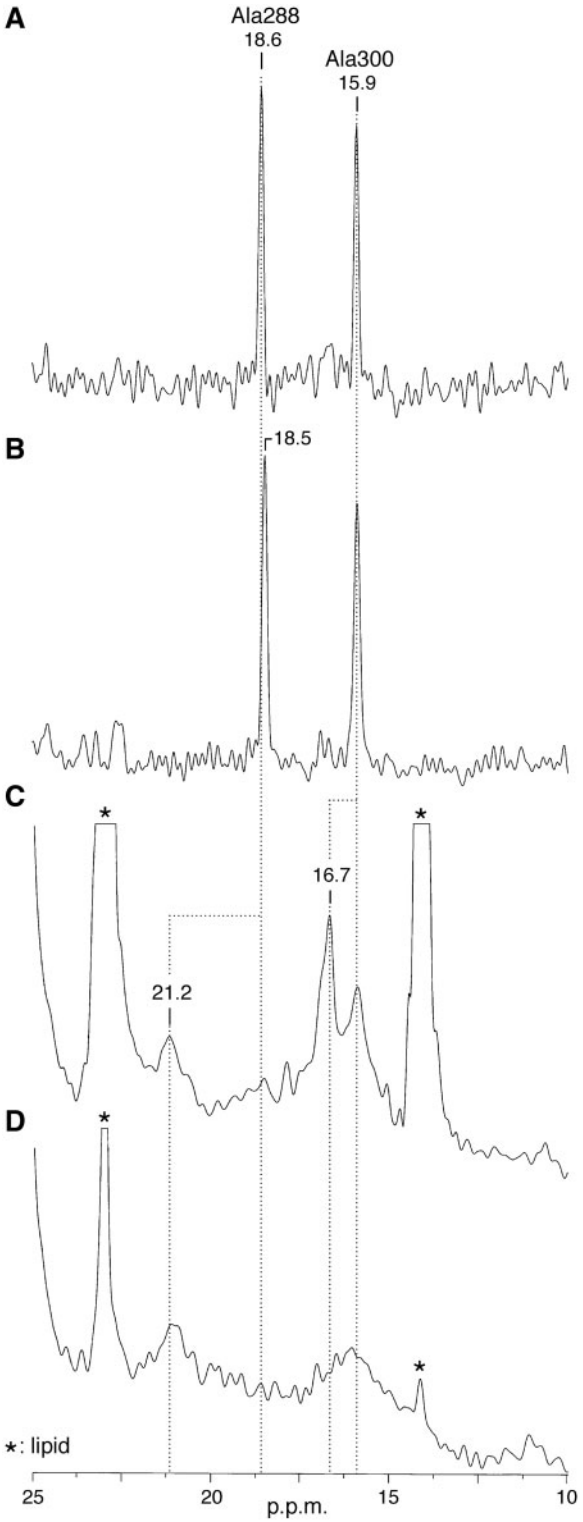

Fig. 5 ^{13}C NMR spectra of the [3-^{13}C]Ala-labelled SWAP-70 PH domain. (A) Unliganded PH domain in solution. The concentration of PH domain is 2.33 mM. (B) PH domain complexed with Ins(1,3,4,5)P_4 in solution. The concentrations of PH domain and Ins(1,3,4,5)P_4 are 2.33 and 2.66 mM, respectively. (C) DD-MAS and (D) CP-MAS ^{13}C NMR spectra of the PH domain bound to PtdIns(3,4,5)P_3 embedded in POPC/PtdIns(3,4,5)P_3 vesicles. The concentrations of PH domain and PtdIns(3,4,5)P_3 are ~4.3 and 11 mM, respectively. The asterisks indicate signals from lipid molecules.

residues in the α-helix appears at ~15 ppm, and the Ala residues in the β-sheet appear downfield at ~19 ppm. The signal of the residue in the disordered random coil structure appears ~16.9 ppm. According to the conformation-dependent chemical shift, the peaks at 21.2 ppm in Fig. 5C and D are ascribed to an Ala residue in the β-sheet. The chemical shift of the peak at 16.7 ppm coincides with the chemical shift of the random coil structure. In the CP-MAS spectrum (Fig. 5D), the peak at 16.7 ppm is suppressed. In the DD-MAS spectrum, the signal intensity is proportional to number of observed ^{13}C nuclei, since ^{13}C nuclei are uniformly excited by the radio frequency pulse tuned to the resonance frequency of ^{13}C nuclei. In contrast, in the case of the CP-MAS spectrum, ^{1}H nuclei are excited first, and ^{13}C nuclei are then excited indirectly through magnetization transfer (cross-polarization) from ^{1}H to ^{13}C nuclei. Since the magnetic dipolar interaction responsible for the cross-polarization between ^{1}H and ^{13}C nuclei is averaged out by rapid reorientation of the internuclear vector between ^{1}H and ^{13}C nuclei, ^{13}C signals from mobile portions of the protein, such as disordered structures will be suppressed in the CP-MAS spectrum. This indicates that the peak at 16.7 ppm in Fig. 5C originates from an Ala residue in a mobile disordered random coil structure. Assignments of these peaks of the vesicle-bound PH domain were attempted after performing site-directed replacement of Ala residues by Gly residues. These attempts were unsuccessful due to serious perturbations of the PH domain structure, which occurred as a result of the mutations. In the model structure (Fig. 1), Ala288 is located at the C-terminus of the β7-strand. As shown in Fig. 1B, the C-terminus of the β7-strand is included in the centre of the β-sheet consists of β1, β2, β7, β6 and β5-strands, which connects two sheets of the β-sandwich to provide frameworks for the core structure and the canonical lipid-binding site of the SWAP-70 PH domain. According to this structural importance, the C-terminus of the β7-strand in the vicinity of Ala288 unlikely changes into the mobile disordered structure without serious perturbation of the structure and function of the PH domain. On the contrary, the C-terminal region of the PH domain involving Ala300 is expected to be able to unfold without deformation of the core structure. Taking into account of these characteristics of Ala288 and Ala300 in the model structure and conformation-dependent chemical shifts, we assigned the peak at 16.7 ppm to a disordered conformation of Ala300 and the peak at 21.2 ppm to a modified β-sheet conformation of Ala288.

Influence of the ether lipids on the structure of the SWAP-70 PH domain at the vesicle surface

In order to observe ^{13}C NMR spectra of ^{13}C-labelled carbonyl carbons of the Trp residues in the absence of interference from natural abundance ^{13}C peaks of the lipid carbonyl groups, an ether lipid (Di-*O*-DMPC) lacking the acyl chain carbonyl groups was substituted for POPC in the PtdIns(3,4,5)P_3-containing vesicles. Figure 6A and B shows the DD-MAS and CP-MAS

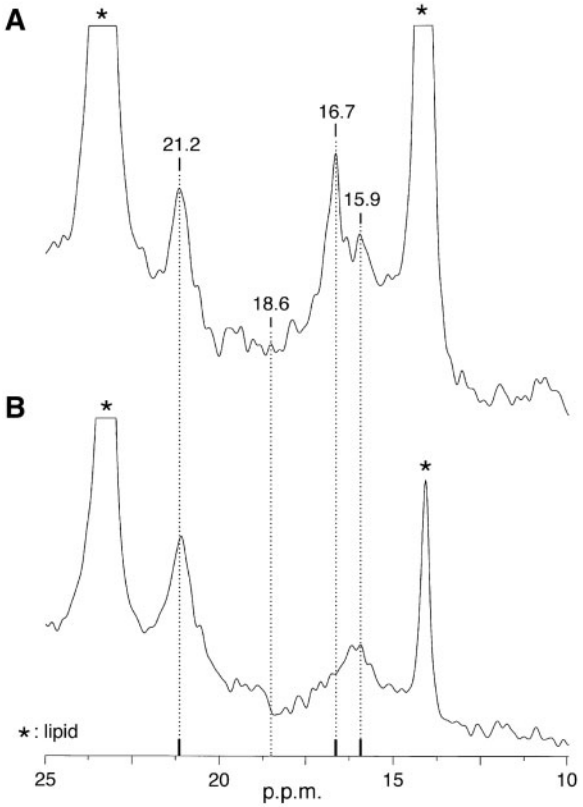

Fig. 6 ^{13}C NMR spectra of the [3-^{13}C]Ala-labelled SWAP-70 PH domain bound to Di-*O*-DMPC/PtdIns(3,4,5)P_3 vesicles. (A) DD-MAS and (B) CP-MAS ^{13}C NMR spectra of the PH domain bound to PtdIns(3,4,5)P_3 embedded in Di-*O*-DMPC/PtdIns(3,4,5)P_3 vesicles. The concentrations of PH domain and PtdIns(3,4,5)P_3 are ~4.3 and 11 mM, respectively. Chemical shifts of the peaks observed for the PH domain bound to PtdIns(3,4,5)P_3 in POPC/PtdIns(3,4,5)P_3 vesicles are indicated with vertical bars. The asterisks indicate signals from lipid molecules.

^{13}C NMR spectra of the [3-^{13}C]Ala-labelled SWAP-70 PH domain bound to the Di-*O*-DMPC/PtdIns(3,4,5)P_3 vesicles. The chemical shifts of the [3-^{13}C]Ala-labelled PH domain bound to the POPC/PtdIns(3,4,5)P_3 vesicles are indicated by vertical bars at the bottom of the spectra. Both of the DD-MAS and CP-MAS spectra of the PH domain bound to the Di-*O*-DMPC/PtdIns(3,4,5)P_3 vesicles are similar to those of the PH domain bound to POPC/PtdIns(3,4,5)P_3 vesicles (Fig. 5C and 5D). Increases in intensity of the peaks at 21.2 ppm accompanied by decreases in intensity at 18.6 ppm, which correspond to the chemical shift of Ala288 in solution, were induced by the lipid substitution of Di-*O*-DMPC. This indicates that the conformational alteration of Ala288 in the PH domain induced at the vesicle surface is marginally facilitated by Di-*O*-DMPC.

^{13}C NMR spectra of the [1-^{13}C]Trp-labelled SWAP-70 PH domain

Figure 7A shows ^{13}C NMR spectra of the unliganded [1-^{13}C]Trp-labelled SWAP-70 PH domain in solution. The ^{13}C-labelled main chain carbonyl groups of three tryptophan residues, Trp227, Trp231 and Trp297, give rise to well-resolved narrow peaks of equal intensities

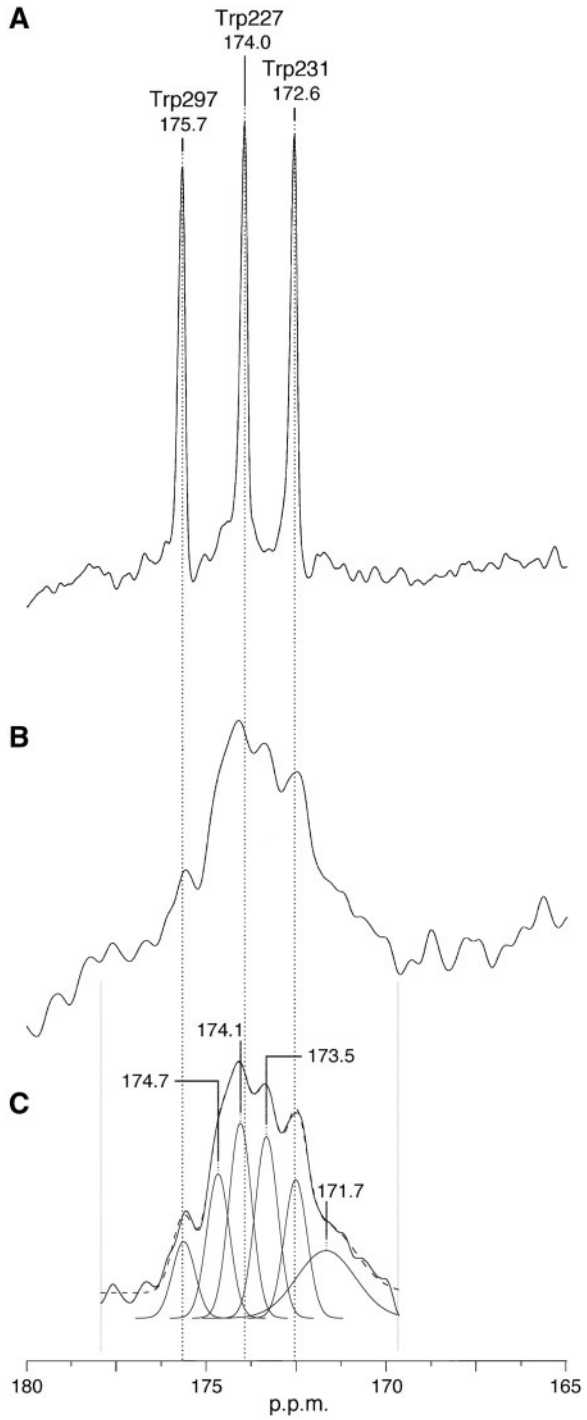

Fig. 7 ^{13}C NMR spectra of the [1-^{13}C]Trp-labelled SWAP-70 PH domain. (A) Unliganded PH domain in solution. (B) DD-MAS ^{13}C NMR spectra of the PH domain bound to PtdIns(3,4,5)P_3 embedded in Di-*O*-DMPC/PtdIns(3,4,5)P_3 vesicles. Concentrations of PH domain and PtdIns(3,4,5)P_3 are ~4.3 and 11 mM, respectively. (C) Deconvolution of the spectrum shown in the (B). The original spectrum and gaussian curves obtained by the deconvolution are shown by solid lines. An envelope of the sum of the gaussian curves is shown by a dashed line.

at 174.0, 172.6 and 175.7 ppm, respectively. The assignments of the Trp residues are based on the reported assignments of the ^{13}C NMR spectrum (BMRB # 10319). In the model structure, Trp297 is located at the centre of the C-terminal α-helix, and Trp227 and Trp231 are located at the N-terminus and the centre of the β2-strand, respectively (Fig. 1B). Figure 7B shows the DD-MAS ^{13}C NMR spectrum of the [1-^{13}C]Trp-labelled PH domain bound to the Di-*O*-DMPC/PtdIns(3,4,5)P_3 vesicles. Four peaks at 172.6, 173.5, 174.1 and 175.7 ppm and a shoulder at 174.7 ppm are resolved. A result of a deconvolution of the DD-MAS spectrum in Fig. 7B is shown in Fig. 7C. An inhomogeneous broad signal from natural abundance ^{13}C nuclei in the carbonyl groups, which appears between 169 and 174 ppm was represented by a broad gaussian curve centred at 171.7 ppm. The rest of the spectrum could be deconvoluted into five gaussian curves with line width of 45 Hz. The chemical shifts of the gaussian curves at 172.6, 174.1 and 175.7 ppm coincide with the peaks of Trp231, Trp227 and Trp297 in the unliganded PH domain in solution (Fig. 7A), respectively. The gaussian curves at 173.5 and 174.7 ppm for the vesicle-bound state have no corresponding peaks in the spectrum of the unliganded state (Fig. 7A). A significantly low relative intensity of the gaussian curve at 175.7 ppm in the vesicle-bound state (Fig. 7C) compared with the peak at 175.7 ppm in the unliganded state (Fig. 7A) indicates an upfield shift of the signal of Trp297 from 175.7 ppm in the unliganded state to 173.5 or 174.7 ppm in the vesicle-bound state of the PH domain.

Discussion

As summarized in Table I, the SWAP-70 PH domain shows K_d's of 2.65 and 12.6 μM for PtdIns(3,4,5)P_3 and PtdIns(4,5)P_2 embedded in the POPC vesicles, respectively. In the absence of the phosphoinositides, binding affinity of the PH domain to the POPC vesicles was not detectable. These results indicate that the SWAP-70 PH domain not only recognizes the head group of PtdIns(3,4,5)P_3 in POPC vesicles, but also possesses affinity for PtdIns(4,5)P_2. Whereas SWAP-70 has been reported to be recruited from the cytoplasm to the plasma membrane in response to the cell stimulation via affinity of the PH domain for PtdIns(3,4,5)P_3, a version of SWAP-70 that lacks a short C-terminal fragment, was shown to be localized to the plasma membrane in a manner that was independent of the stimulation conditions (*13*, *19*). The rather high affinity of the SWAP-70 PH domain for both PtdIns(3,4,5)P_3 and PtdIns(4,5)P_2 is consistent with the nature of SWAP-70 in the cell. This suggests that although the affinity of PH domain for phosphoinositides provides a driving force for membrane localization of SWAP-70, the binding selectivity for PtdIns(3,4,5)P_3 is provided by another part of the protein.

The CD and fluorescence spectra of the SWAP-70 PH domains in the presence of POPC vesicles or bound to Ins(1,3,4,5)P_4 agree with the spectra of the unliganded PH domain in solution (Figs 3A, B and 4A). ^{13}C NMR spectra of Ala288 and Ala300 are also indifferent to the binding of Ins(1,3,4,5)P_4 (Fig. 5A and B). These results indicate that the non-specific interaction with the POPC lipid bilayer and binding of Ins(1,3,4,5)P_4 do not affect the conformation of the

SWAP-70 PH domain. In contrast, the CD and fluorescence spectra reveal that the secondary structure and the local environment of the Trp residues of the PH domain bound to the phosphoinositides in vesicles are different from those of the unliganded PH domain (Figs 3B, 4B and C). Increases in the negative values at ~232 nm and at wavelengths <210 nm in the CD spectra indicate a conformational alteration of the β-sandwich and formation of the disordered random coil structure in the vesicle-bound state, respectively. The changes in the fluorescence spectra indicating alterations of local environment in the vicinity of Trp residues coincide with these conformational alterations. The conformational changes occurring in the vesicle-bound state, which are detected by CD spectroscopy are suppressed by coexistence of Ins(1,3,4,5)P_4 (Fig. 3C). In addition, the CD spectra in Fig 3B and C appear to have an isodichroic point at 222 nm. This suggests that the two different structures of the PH domain corresponding to the unliganded or Ins(1,3,4,5)P_4-bound state and the vesicle-bound state undergo reversible interconversion. The characteristics of the vesicle-bound PH domain observed by CD and fluorescence spectroscopy are virtually identical for the vesicles containing PtdIns(4,5)P_2 and PtdIns(3,4,5)P_3 (Figs 3B and 4B). This indicates that the anchoring of the PH domain to the lipid bilayer surfaces by either PtdIns(4,5)P_2 or PtdIns(3,4,5)P_3 produces the same structure of the PH domain. The ^{13}C NMR spectra of the ^{13}C-labelled Ala and Trp residues in the PH domain bound to the PtdIns(3,4,5)P_3 vesicles show details of the conformational alterations at the positions of these residues (Figs 5, 6 and 7). The downfield shift of the Ala288 signal to 21.2 ppm indicates conformational modification of the β7-strand, and the shift of the Ala300 signal from 15.9 to 16.7 ppm reveals the conformational transition of the C-terminal α-helix to the mobile random coil structure (Fig. 5C and D). The structural change of Trp297 detected by the upfield shift of the ^{13}C NMR signal (Fig. 7B and C) also supports the conformational transition of the C-terminal α-helix, which involves Trp297 at the centre of the helix. These characteristics in the conformational alterations agree with those detected by CD spectroscopy. This indicates that the SWAP-70 PH domain undergoes conformational changes that include the transition of the C-terminal α-helix to the mobile random coil structure when the PH domain binds to the phosphoinositide embedded in the lipid bilayer vesicles.

These findings of the conformational alterations of the SWAP-70 PH domain induced at the lipid bilayer surface would provide a regulatory mechanism of the SWAP-70 function related to the intracellular location of the protein. As shown in Fig. 1B, the C-terminal α-helix of the SWAP-70 PH domain contains an NLS. The series of four Lys residues of the NLS (Lys291—Lys294) are shown to be required for the nuclear localization of SWAP-70 in the cell. The X-ray model structures of complexes of nuclear import receptor importin-α and NLS peptides reveal that the NLS peptides adopt extended conformations in the complexes (*24*, *25*). The conformational transition of the C-terminal α-helix to form a disordered structure presented in this study would enable a water-exposed, extended form of NLS and is likely to facilitate formation of the nuclear transport complex. In the stimulated B lymphocytes, SWAP-70 has been shown to be translocated from the cytoplasm to the plasma membrane in response to the PtdIns(3,4,5)P_3 production by the activated phosphatidylinositol 3-kinase, and then transported to the nucleus by importins (*13*). The conformational transition of the C-terminal α-helix of the SWAP-70 PH domain caused by the recognition of the phosphoinositides in the membrane could provide a switching mechanism for the

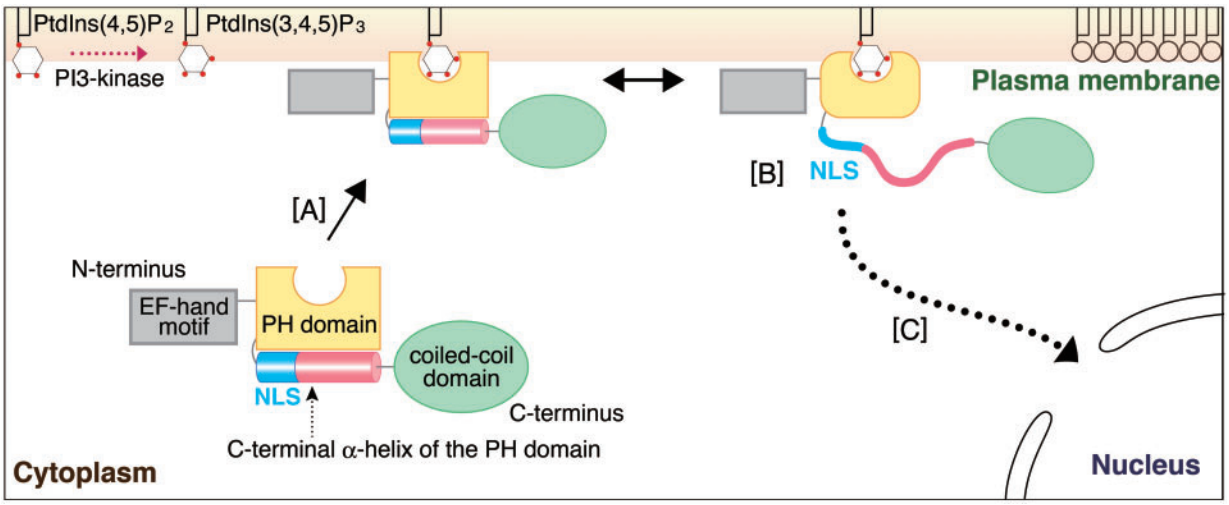

Fig. 8 A possible mechanism for the intracellular re-localization of SWAP-70. When PtdIns(3,4,5)P_3 is produced in the plasma membrane as a result of cell stimulation, unliganded SWAP-70 in the cytoplasm is recruited to the plasma membrane. The PH domain is anchored to the head group of phosphoinositide in the membrane [A]. The interaction between the membrane and the PH domain induces conformational alterations including unfolding of the C-terminal α-helix [B]. As a result of the conformational transition of the C-terminal α-helix, the NLS in the α-helix is allowed to form a water-exposed extended conformation, and becomes recognizable by nuclear import receptor, importin-α. After removal from the plasma membrane, SWAP-70 bound to importin-α through the extended NLS is transported into the nucleus [C].

sequential relocalization of SWAP-70 from the plasma membrane to the nucleus, through the unwinding and exposure of the NLS in the C-terminal α-helix at the membrane surface. A hypothetical model for the role of the SWAP-70 PH domain in the intracellular relocalization of SWAP-70 is schematically shown in Fig. 8. Specific high-affinity binding of the C-terminal region of SWAP-70 to non-muscle F-actin has been reported to be required in order to induce membrane ruffling that is stimulated by growth factors (*5*). This interaction between the C-terminus of SWAP-70 and F-actin is proposed to be masked in an unstimulated state. The conformational transition of the C-terminus of the SWAP-70 PH domain at the lipid bilayer surface may also induce exposure of the F-actin-binding site and trigger phosphatidylinositol 3-kinase-dependent co-localization of SWAP-70 with F-actin in the stimulated cells.

Although the structural motif of the PH domain is seems to provide stable structural scaffolds for a number of proteins in solution, the results of the present study suggest that the conformations of those PH domains can be altered at the membrane surface. The structural information on the membrane-bound state of the domains provided by the spectroscopic methods would be required to understand the intracellular location-specific functions of the membrane-binding proteins.

Funding
Ministry of Education, Culture, Sports, Science and Technology of Japan (22570191 to S.T.).

Conflict of interest
None declared.

References

1. Borggrefe, T., Wabl, M., Akhmedov, A.T., and Jessberger, R. (1998) A B-cell-specific DNA recombination complex. *J. Biol. Chem.* **273**, 17025–17035
2. Gross, B., Borggrefe, T., Wabl, M., Sivalenka, R.R., Bennett, M., Rossi, A.B., and Jessberger, R. (2002) SWAP-70-deficient mast cells are impaired in development and IgE-mediated degranulation. *Eur. J. Immunol.* **32**, 1121–1128
3. Hilpela, P., Oberbanscheidt, P., Hahne, P., Hund, M., Kalhammer, G., Small, J.V., and Bahler, M. (2003) SWAP-70 identifies a transitional subset of actin filaments in motile cells. *Mol. Biol. Cell* **14**, 3242–3253
4. Ocana-Morgner, C., Wahren, C., and Jessberger, R. (2009) SWAP-70 regulates RhoA/RhoB-dependent MHCII surface localization in dendritic cells. *Blood* **113**, 1474–1482
5. Ihara, S., Oka, T., and Fukui, Y. (2006) Direct binding of SWAP-70 to non-muscle actin is required for membrane ruffling. *J. Cell. Sci.* **119**, 500–507
6. Pearce, G., Angeli, V., Randolph, G.J., Junt, T., von Andrian, U., Schnittler, H.J., and Jessberger, R. (2006) Signaling protein SWAP-70 is required for efficient B cell homing to lymphoid organs. *Nat. Immunol.* **7**, 827–834
7. Sivalenka, R.R. and Jessberger, R. (2004) SWAP-70 regulates c-kit-induced mast cell activation, cell-cell adhesion, and migration. *Mol. Cell. Biol.* **24**, 10277–10288
8. Liu, J., Li, D., Cao, B., Li, Y.X., Herva, R., Piao, Y.S., and Wang, Y.L. (2007) Expression and localization of SWAP-70 in human fetomaternal interface and placenta during tubal pregnancy and normal placentation. *J. Histochem. Cytochem.* **55**, 701–708
9. Seol, H.J., Smith, C.A., Salhia, B., and Rutka, J.T. (2009) The guanine nucleotide exchange factor SWAP-70 modulates the migration and invasiveness of human malignant glioma cells. *Transl. Oncol.* **2**, 300–309
10. Fukui, Y., Tanaka, T., Tachikawa, H., and Ihara, S. (2007) SWAP-70 is required for oncogenic transformation by v-Src in mouse embryo fibroblasts. *Biochem. Biophys. Res. Commun.* **356**, 512–516
11. Murugan, A.K., Ihara, S., Tokuda, E., Uematsu, K., Tsuchida, N., and Fukui, Y. (2008) SWAP-70 is important for invasive phenotypes of mouse embryo fibroblasts transformed by v-Src. *IUBMB Life* **60**, 236–240
12. Fukui, Y. and Ihara, S. (2010) A mutant of SWAP-70, a phosphatidylinositoltrisphosphate binding protein, transforms mouse embryo fibroblasts, which is inhibited by sanguinarine. *PLoS One*. **5**, e14180
13. Masat, L., Caldwell, J., Armstrong, R., Khoshnevisan, H., Jessberger, R., Herndier, B., Wabl, M., and Ferrick, D. (2000) Association of SWAP-70 with the B cell antigen receptor complex. *Proc. Natl. Acad. Sci. USA* **97**, 2180–2184
14. Rebecchi, M.J. and Scarlata, S. (1998) Pleckstrin homology domains: a common fold with diverse functions. *Annu. Rev. Biophys. Biomol. Struct.* **27**, 503–528
15. Lemmon, M.A. and Ferguson, K.M. (2000) Signal-dependent membrane targeting by pleckstrin homology (PH) domains. *Biochem. J.* **350 (Pt 1)**, 1–18
16. Maffucci, T. and Falasca, M. (2001) Specificity in pleckstrin homology (PH) domain membrane targeting: a role for a phosphoinositide-protein co-operative mechanism. *FEBS Lett.* **506**, 173–179
17. Lemmon, M.A., Ferguson, K.M., and Abrams, C.S. (2002) Pleckstrin homology domains and the cytoskeleton. *FEBS Lett.* **513**, 71–76
18. Lemmon, M.A. (2003) Phosphoinositide recognition domains. *Traffic* **4**, 201–213
19. Wakamatsu, I., Ihara, S., and Fukui, Y. (2006) Mutational analysis on the function of the SWAP-70 PH domain. *Mol. Cell. Biochem.* **293**, 137–145
20. Uekama, N., Sugita, T., Okada, M., Yagisawa, H., and Tuzi, S. (2007) Phosphatidylserine induces functional and structural alterations of the membrane-associated pleckstrin homology domain of phospholipase C-δ1. *FEBS J.* **274**, 177–187
21. Marinetti, G.V. (1962) Chromatographic separation, identification, and analysis of phosphatides. *J. Lipid Res.* **3**, 1–20
22. Saito, H., Tuzi, S., Yamaguchi, S., Tanio, M., and Naito, A. (2000) Conformation and backbone dynamics of bacteriorhodopsin revealed by ^{13}C-NMR. *Biochim. Biophys. Acta.* **1460**, 39–48
23. Ando, I., Asakawa, N., and Webb, G.A (1998) NMR chemical shift and electronic structure in *Solid State NMR of Polymers* (Asakura, T. and Ando, I., eds.), pp. 1–21, Elsevier, Amsterdam
24. Fontes, M.R., Teh, T., and Kobe, B. (2000) Structural basis of recognition of monopartite and bipartite nuclear localization sequences by mammalian importin-α. *J. Mol. Biol.* **297**, 1183–1194
25. Hodel, M.R., Corbett, A.H., and Hodel, A.E. (2001) Dissection of a nuclear localization signal. *J. Biol. Chem.* **276**, 1317–1325